

Supplemental Figures

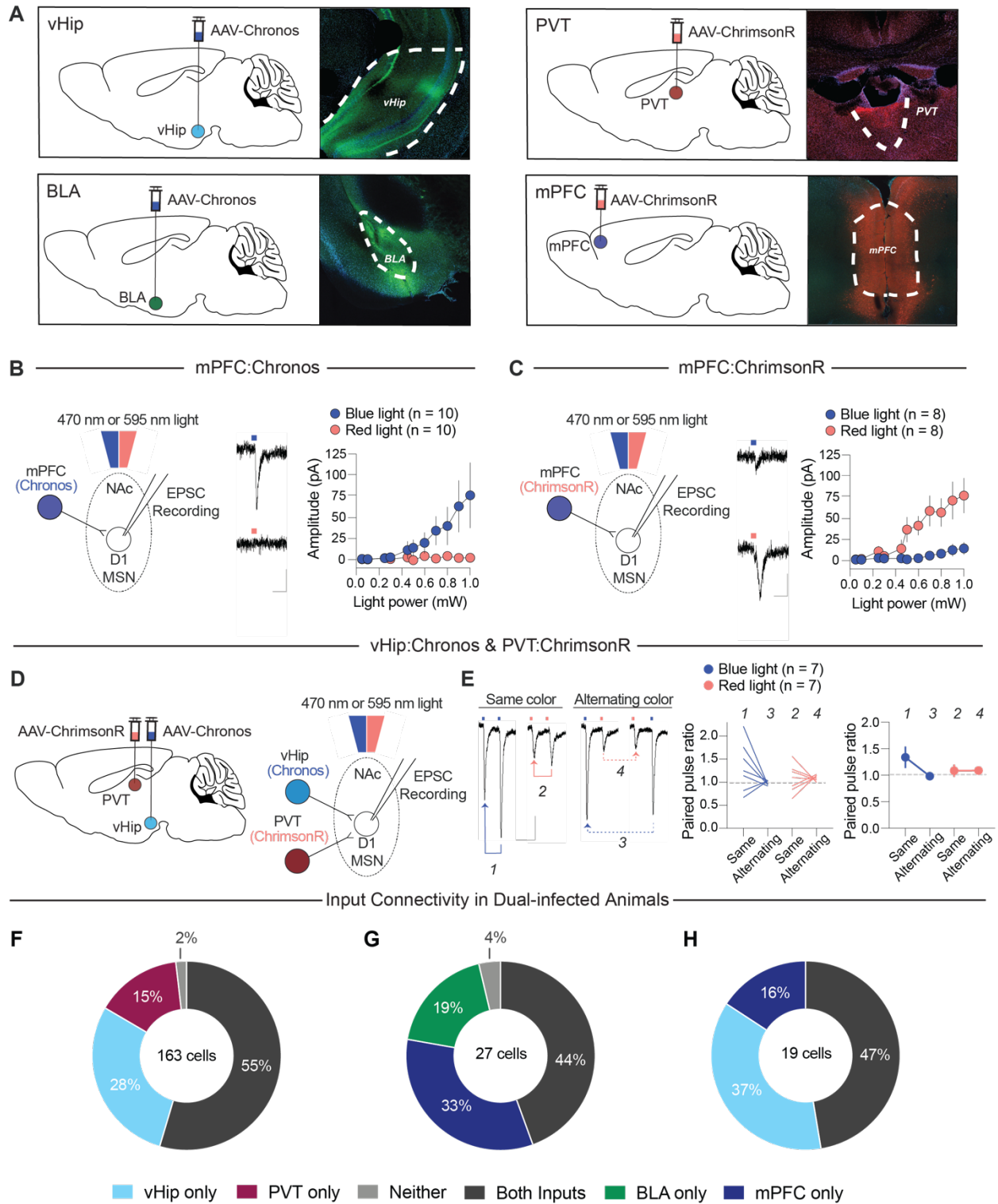


Figure S1. Optogenetic Strategy for Studying NAc Inputs

(A) Schematic of AAV targeting to different brain regions, showing typical expression patterns of Chronos and ChrimsonR. Scale bar (lower right) = 1 mm for all images. (B) Left: Schematic of whole-cell recording in NAc with sample EPSCs from 1 mW blue (upper trace) or red (lower trace) 5 ms LED pulses for Chronos-mPFC infected mice. Scale bars: 20 ms / 20 pA. Right: EPSC amplitudes (mean \pm SEM) from mPFC input stimulation as a function of light power from Chronos-mPFC mice. (C) Same as (B), except for ChrimsonR-mPFC infected mice. (D) Schematics showing injection (left) and whole-cell recording (right) strategies for dual infected mice. (E) Sample EPSCs in response to paired-pulse stimulation (left) and corresponding quantification showing individual cells (left graph) and summary (mean \pm SEM; right graph) for dual-infected mice. Scale bars: 50 ms / 50 pA. (F) Proportion of NAc D1-MSNs in which EPSCs were generated in recordings from animals dually infected in vHip and PVT with Chronos and ChrimsonR, respectively. "Only" indicates the percentage of cells with measurable EPSCs from only one of the two inputs despite sufficient expression of both opsins in the animal. (G) Same as (F), but for dual-infected BLA (Chronos) and mPFC (ChrimsonR) animals. (H) Same as (F), but for dual-infected vHip (Chronos) and mPFC (ChrimsonR) animals.

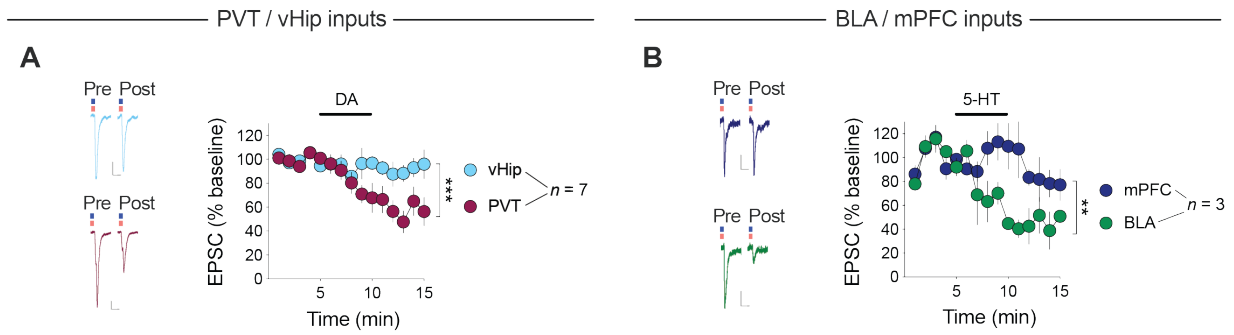


Figure S2. Effects of DA and 5-HT in Single Cells on Which Two Inputs Converged

(A) Left: Sample vHip→NAc EPSCs (top) and PVT→NAc EPSCs (bottom) pre- and post-DA recorded in the same neuron using two different opsins. Right: Summary time course of effects of DA ($F_{14,168} = 3.076$, $P < 0.001$). Scale bars: 20 ms / 20 pA. (B) Same as (A) but for mPFC→NAc (top) and BLA→NAc (bottom) EPSCs pre- and post-5-HT ($F_{14,56} = 2.529$, $P < 0.01$). Mean \pm SEM. ** $P < 0,01$, *** $P < 0.001$; two-way ANOVA with Sidak's multiple comparison post hoc test.

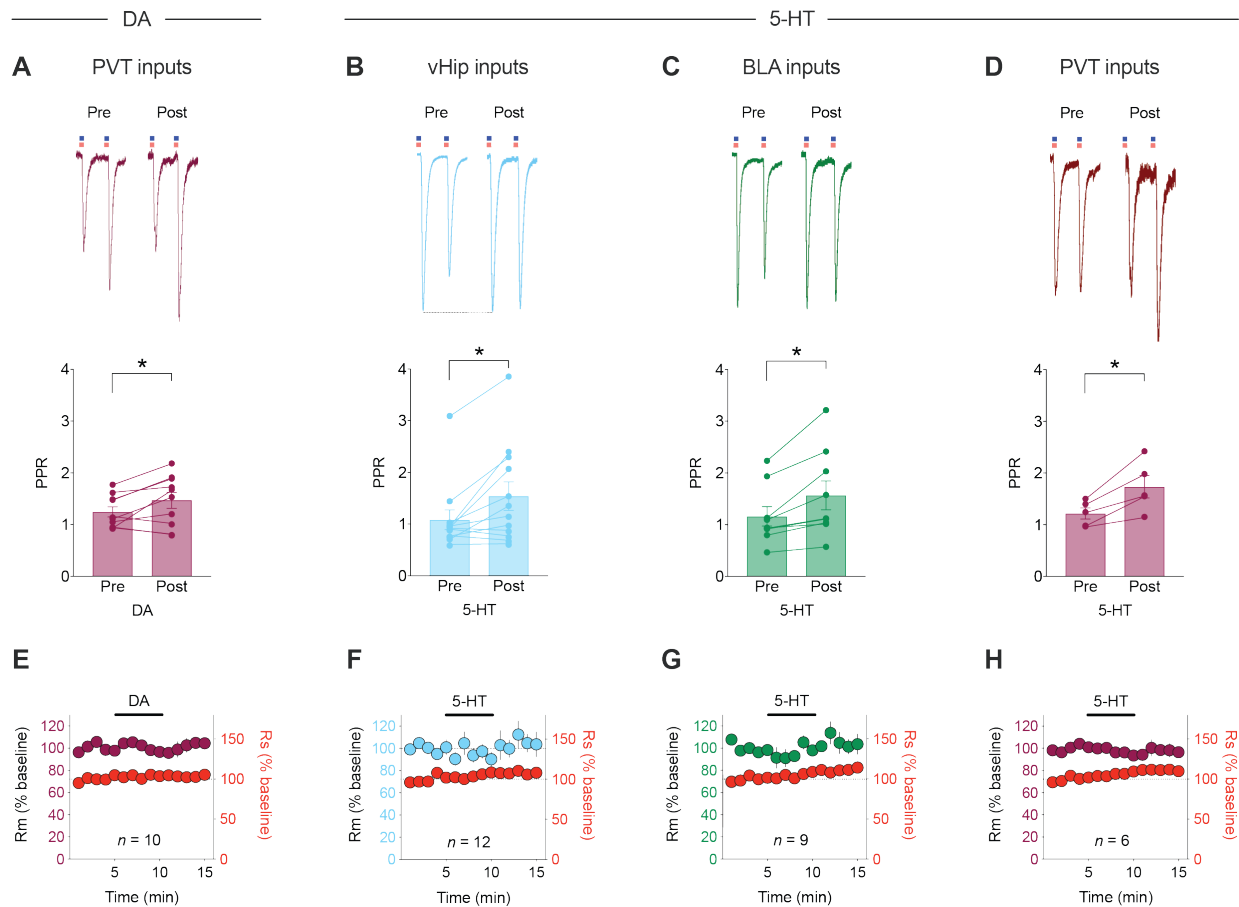


Figure S3. PPR, Rm, and Rs for Recordings in Inputs Affected by DA or 5-HT

(A) Top: sample PVT→NAc EPSCs pre- and post-DA showing responses to paired-pulse light pulses at 50 ms interval (scaled to pre EPSC₁). Bottom: average and individual PPRs for PVT-derived EPSCs pre- and post-DA. ($t=2.373$, $df=9$). Student's two-tailed paired t test. (B-D) Same as (A) but for 5-HT acting on inputs from vHip (B, $t=3.106$, $df=11$), BLA (C, $t=3.622$, $df=8$), or PVT (D, $t=4.087$, $df=4$). Mean \pm SEM. * $P<0.05$. Student's two-tailed paired t test. (E) Membrane resistance (Rm) and series resistance (Rs) (mean \pm SEM) for PVT→NAc EPSC recordings. (F-H) Same as (E) but for neurons exposed to 5-HT during activation of inputs from vHip (F), BLA (G), or PVT (H).

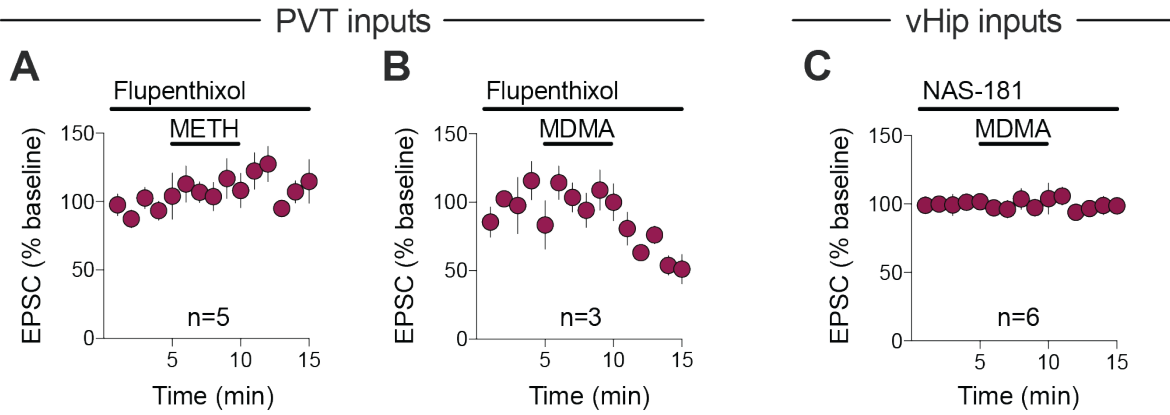


Figure S4. DA and 5-HT_{1b} Receptor Antagonists Block Input-specific Depression of Excitatory Transmission by METH and MDMA. Continuous flupenthixol application blocks the effect of (A) METH, but not (B) MDMA on PVT→NAc D1-MSN EPSCs. Continuous NAS-181 application blocks the effect of (C) MDMA on vHip→NAc D1-MSN EPSCs.

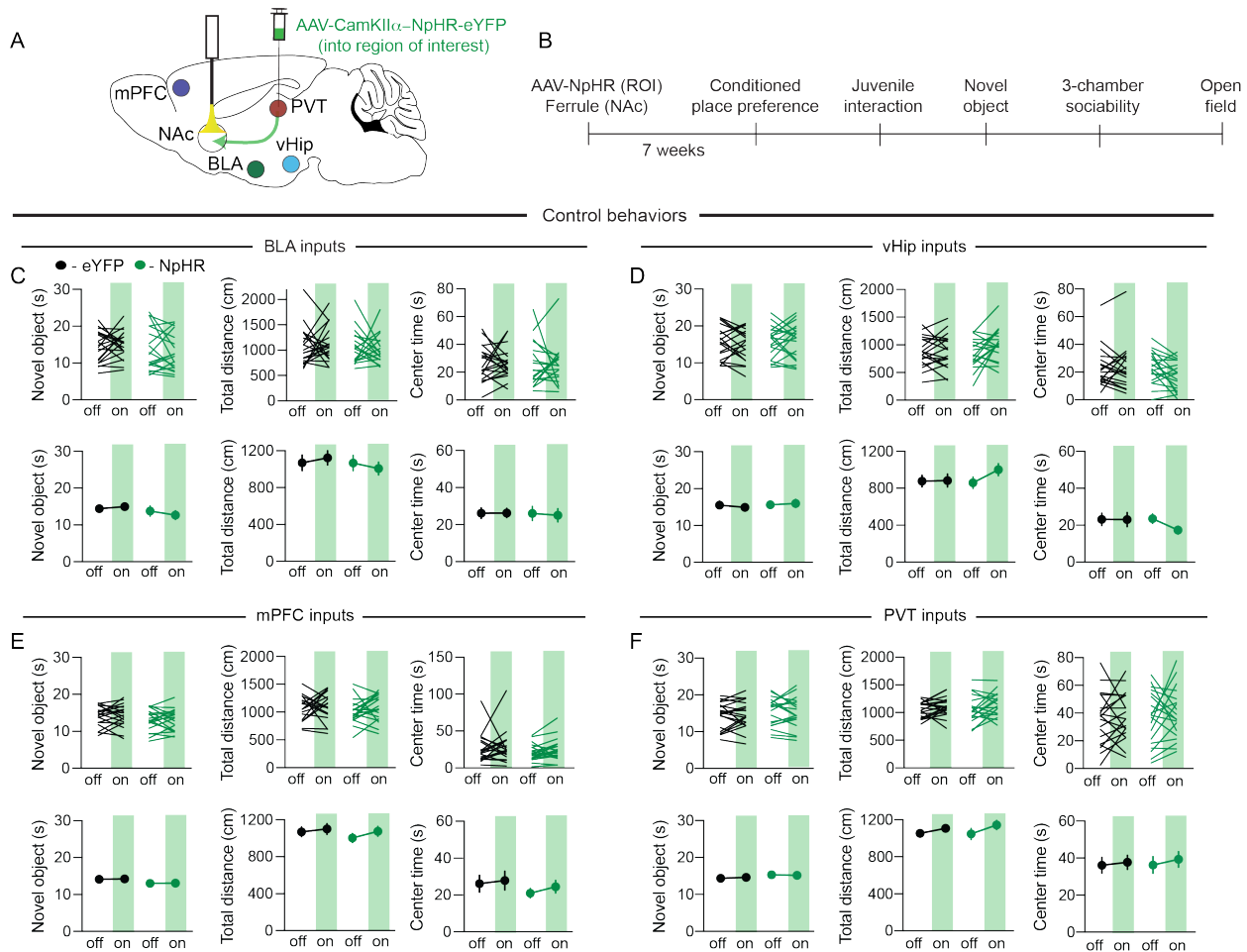


Figure S5. Consequences of Input-specific Inhibition in NAc on Control Behaviors

(A) Schematic of AAV targeting to different brain regions of interest and fiber implant in the NAc.

(B) Timeline of behavioral assays. (C-F) Effects of inhibition of BLA, vHip, mPFC, and PVT

inputs to NAc on novel object, locomotion, and center time.